Intermediate band for solar cells. Transition metals supersaturated Silicon approach

G. González-Díaz , E. García-Hemme , R. García-Hernansanz , J. Olea , D. Pastor , A. del Prado , I. Mártil , P. Wahnón

Abstract— **Within the framework of the third solar cell generation some new ideas to enlarge the spectral response of the solar cells toward the infrared have been proposed. Among them the inclusion of an Intermediate Band (IB) seems to be very promising. This paper will deal with one of the ways to generate the IB namely the deep level center approach. We will discuss not only its existence but also the carriers lifetime recovery which is necessary to obtain the expected increase of the solar cell efficiency.**

Keywords—Titanium, vanadium, silicon, ion implantation, pulsed laser melting, intermediate band, solar cells.

I.- AN INTRODUCTION TO THE INTERMEDIATE BAND SOLAR CELL

The problem of renewable energy sources is a commonplace now. In this paper we will deal with photovoltaic energy, i.e. the direct conversion of solar radiation to electrical energy. This is also a commonplace and we are assuming the change in the landscape made by the solar cell farms. Being, as I am, a proud supporter of the photovoltaic energy I must accept that the real state it takes is unacceptable. Of course the only solution is to increase the efficiency, at least for terrestrial use.

It is well known that the limited efficiency of a solar cell is produced by a basic tradeoff. If we use a high gap semiconductor like GaAs as an example, we will obtain a high voltage solar cell but we will profit only from those photons having energy higher than the semiconductor bandgap. As a consequence we will have a limited current and a limited power output, i. e. a limited efficiency. Conversely, if we use a low bandgap semiconductor, like Ge, we will take advantage of the complete solar spectrum absorbing most of the photons reaching the cell, but we will obtain a small output voltage and also a limited efficiency.

This basic tradeoff has been known from the start of the solar cell in the seventies, and was theoretically studied by numerous authors that guessed the optimum gap for the highest efficiency.

The most efficient solution known until now is the tandem solar cell. As a high gap semiconductor is transparent to photons with lower energy than the gap we can arrange a stack of cells placing the high gap semiconductor cell on top and the lower gap semiconductor at the bottom. If the cells are accurately designed to produce the same current we can obtain a output voltage which will be the sum of the one in each cell. A basic problem complicates this theoretically simple scheme: if the stack is made with cells N-P/N-P etc we will have a reverse PN junction in between each cell that will drastically limit the current. To avoid this problem a tunnel junction between cells is mandatory.

It is clear that the complex technology of the tandem solar cell could not be a solution for the energy challenge, at least for now. In 1997 (1) a striking proposal was put forward to of the scientific community by prof. Luque from the Politechnical University of Madrid: could it be possible to build a cell that mimicked the basic principles of a tandem solar cell, but without the drawback of the tunnel diodes?. That would be possible if we had a material with the ability to absorb both the low energy and the high energy photons though having an output voltage similar to the cells that only absorb high energy photons. These contradictory requirements could be fulfill if we envisaged a semiconductor with an intermediate band as the one depicted in fig 1.

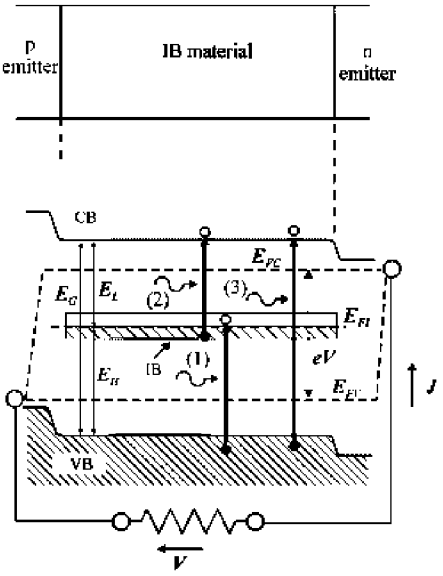

Fig 1: Electronic diagram of an Intermediate band solar cell (IBSC)

Imagine a semiconductor, silicon as an example, in which we have added an extra band in between the Valence Band (VB) and the Conduction Band (CB). This band, that we will call the Intermediate Band (IB), has to be semi-filled in order to accept electrons from the VB to the IB when a photon of a minimum energy of E_H impinges in the cell (transition 1). The same thing happens with transition 2. Those transitions are in addition to the normal ones for a solar cell i.e. VB to CB (3).

If the intermediate band is filled, transition 1 is not possible and conversely happens with transition 2 if the IB is empty. This is the way to absorb photons of lower energy than the gap. To produce high output voltage the semiconductor with the IB has to be sandwiched between two "normal" semiconductors, one P type and the other N type.

Theoretical studies predict a maximum efficiency of 63.2% under concentration for the IB solar cell (IBSC). Unfortunately, a semiconductor with three bands as required for an IBSC does not exist in nature and the problem now is to study the feasibility to synthetize it.

II.- IB PRACTICAL IMPLEMENTATION

There are by now three ways to build a IBSC: the quantum dot, the mismatched alloy and the deep levels model. I will talk briefly about two former ones and extensively about the latter. First of all it is important to advance that in the three cases the maximum efficiency obtained is .... % far from, not only the expected efficiency of an IBSC, but also from the conventional solar cells.

In the quantum dot (QD) implementation of an IBSC (QD-IBSC) an array of quantum dots are sandwiched between conventional P and N semiconductors. A QD is an extremely small volume of a semiconductor with lower energy gap than the one of the semiconductor where the dot array is embedded. The size of the dot should be small enough to produce quantification of its energy levels. Moreover, the distance between adjacent dots should be also small to permit an overlapping of the wavefunctions of the electrons taking up the energy levels in the dots (fig 2). In this way an IB is formed at some energy level that is higher than the CB of the lower gap semiconductor and lower than the CB of the higher gap semiconductor.

The highly mismatched alloy approach is related with the modifications that the insertion of a small amount of an element of high electronegativity produces in the band gap of a semiconductor. As a result the conduction band splits into two sub-bands and consequently an IB is formed.

II.A) THE DEEP LEVELS APPROACH

The third approach to the IB starts with the introduction inside of a semiconductor a foreign atom which produces a deep level. To understand the concept of deep level we have to remember that crudely the gap of a semiconductor (i.e. the distance from VB to CB) is not more than the energy needed to liberate an electron from the silicon bond to produce an almost free electron and a hole. A deep level is produced if the included atom has electrons which could be liberated by using almost half the energy than the one used to remove electrons of the silicon or could accept electrons with a similar amount of energy.

The electronic image for a deep level is a localized physical position in the semiconductor network where an energetic level exits. This level can be used for an electron to be promoted from the VB if the level is empty or to promote its electron to the CB if the level is occupied. This is the idea represented in fig 1.

Unfortunately things are not so easy. A deep level could effectively absorb photons with energy lower than the gap promoting electrons from VB to CB in a two-step process, but it is more efficient recombining them. The recombination is the counterpart of the generation i.e. the mechanism that guarantees the equilibrium. Without recombination, the photogeneration will produce an infinite carrier concentration as the times goes. This is the reason because the presence of deep levels in a semiconductor reduces drastically the lifetime of the photocarriers and its concentration. A semiconductor with a low lifetime is useless for solar cell applications and for most of the electronic devices with the exception of switching devices.

If deep levels are introduced in big quantities the wavefunctions of its electrons start to interact (in a similar way as described for QD) and as a consequence of Pauli´s

principle its energetic levels should differentiate creating a band. N. Mott did the first calculation of the needed concentration which is $6x10^{19}cm^{-3}$ for Silicon. This figure is known as Mott limit.

A band like this is exactly what we are looking for an IBSC, except for the very important question of recombination. Based on configuration diagrams the Politechnical group has argued (2) that when the Mott level is surpassed the photocarriers lifetime recovers and enough high value to be useful for an IBSC. This is not generally accepted as some other groups (3,4) argue than to obtain a true lifetime recovery the IB should as wide as the difference between CB and VB energy.

Some groups (5) have calculated the optimum semiconductor gap and the energetic impurity level for a maximum efficiency solar cell, but up to now and based on this technology the IB has been only obtained in Si.

Besides it application to solar cells, the IB could be used easily to build infrared detectors. Important efforts (6) are been carried out to obtain silicon based infrared detectors, mainly supersaturating Si wafers with chalcogenides. This field has a strategic interest and could benefit from the very mature silicon technology.

From a theoretical point of view P. Wahnon et al (7) has proved the possibility of having a half filled band when Ti is incorporated into Si. Ti produces a deep level and is well known as a carrier lifetime killer.

II B).- EXPERIMENTAL DIFFICULTIES IN THE DEEP LEVEL APPROACH

I will detail in this paragraph the most important problems for developing a deep level IB (DL IBSC). For shake of clarity I will describe the case of Ti as foreign atom and Silicon as host crystal.

As stated before, to obtain an IB we have to surpass the Mott level, which is really a very high level of impurities. Most of the atoms that are known to produce deep level in silicon (like Ti, V, Cr and others) have low solubility in the semiconductors. For example the maximum concentration attainable for Ti in Si in equilibrium is about $10^{14}cm^{-3}$ which is about 5 orders of magnitude lower than the required Mott limit to obtain the IB. That tremendous difference precludes the use of equilibrium techniques to introduce the Ti atom. Consequently we have to use non-equilibrium techniques. To introduce the foreign atom we have used ion implantation, technique that has not limit in the atomic concentration of implanted ions. Unfortunately the penalty to pay is the damage of the Si crystalline network that for this level of impurity implantation became amorfized. To recrystallize the sample a non-equilibrium heating process like laser annealing is necessary.

Ultraviolet very energetic pulses coming form an excimer laser melts the sample superficially in nanoseconds. After the pulse ends, the silicon starts to recrystallize starting from the substrate to the surface in a solidifying front that moves very fast. The un-melted substrate is the seed that guarantees a correct regeneration of the Si crystalline structure. That way the Ti atoms have not enough time to aggregate in clusters.

III. EXPERIMENTAL REALIZATION AND CHARACTERIZATION

Samples 1x1 cm^2 in size of n-type Si (111) with a thickness of 300 μm (ρ≈200 Ωcm; μ≈1500 $cm^2V^{-1}s^{-1}$, n≈2.2x10^{13} cm^{-3} at room temperature) were implanted at 32 keV with different transition metals at a doses from 10^{13} - 10^{16} cm^{-2}. Subsequently the implanted samples were PLM processed at energies from 0.6 - 1.4 J/cm^2 with a KrF excimer laser (248 nm) at IPG Photonics. Also, some Si wafer without implantation and Si samples implanted with Si at 170 keV and 10^{16} cm^{-2} were processed by PLM at 1 J/cm^{-2} for comparatives purposes.

Implanted samples have been characterized by ToF-SIMS, TEM, (8) Raman (9) and RBS (10). Figure 2 shows the TEM images and the SIMS profiles for Ti implantation at various doses. It can be seen that at doses of $10^{15}cm^{-2}$ the crystallinity has been fully recovered. For doses until 10^{16} cm^{-2} the annealing is not perfect and the resulting implanted layer becomes policrystalline. Same results hold for Raman spectroscopy. RBS determines clearly that Ti is located in interstitial places. Only a few percent is located in substitutional positions.

Electrical characterization was made at variable temperature (10 – 300 K) placing the samples inside a closed-cycle Janis cryostat. In order to avoid moisture condensation, the cryostat was attached to a vacuum pump. A Keithley SCS 4200 model with four source and measure units was used to perform the sheet resistance and Hall effect measurements with the van der Pauw configuration (Fig 3). A Kepco bipolar current source was used to feed an electromagnet.

Figures 4a and 4b represent the sheet resistance and the mobility of a series of Ti implantation with doses from 10^{14} to $10^{16}cm^{-2}$ and annealed at 0.8 J/cm^2. Also the substrate resistivity and mobility is represented in both

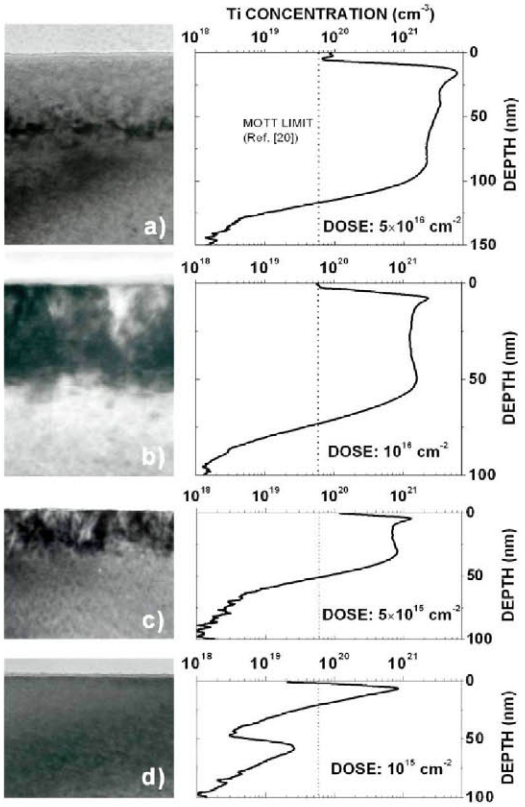

Figure. 2. TEM images and ToF-SIMS profiles of the layers PLM annealed at 0.8 J/cm2 for all the implanted doses. (a) Dose: 5x10^{16} cm^{-2}, (b) dose:10^{16} cm^{-2},(c) dose: 5x10^{15} cm^{-2} and (d) dose:10^{15} cm^{-2}.

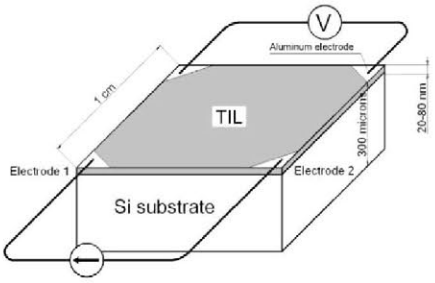

Figure 3: Implanted simple with contacts at the corners to measure the sheet resistance

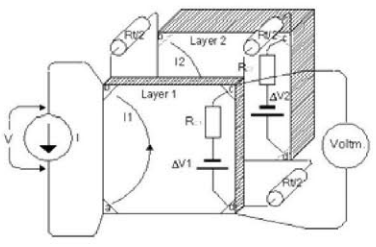

Figure 5: Circuit for the analitycal model

plots. As it can be seen, the electrical properties of the $10^{14}cm^{-2}$ sample are indistinguishable from those of the substrate. Nevertheless sheet resistance for the other doses presents an unconventional behavior. It should be expected that a parallel structure as the one we have should have a sheet resistance lower than that of each one of its branches. In the figure 4a) sheet resistance of the whole sample crosses the sheet resistance of the substrate. Also the behavior of mobility is uncommon.

These behaviors have been simulated with ATLAS framework and also an analytical model has been developed. The model is sketched in fig 5. A current limitation between the implanted layer and the substrate is assumed and it is represented in the picture as Rt. The van der Paw current I is divided between both layers in inverse proportion to the resistances and each layer generates the van der Paw voltage at the opposite terminals. The differential voltmeter reads a voltage which takes into account the resistance seen between the contacts in each layer.

Solving the circuit we can obtain the following equations for the sheet resistance and mobility:

$$R_{sheet} = \frac{G_{C1}+G_{C2}F^2}{\alpha(G_{C1}+G_{C2}F)^2} \qquad [1]$$

$$\mu_{eff} = \frac{\mu_1 G_{C1}+\mu_2 G_{C2}F^2}{G_{C1}+G_{C2}F^2} \qquad [2]$$

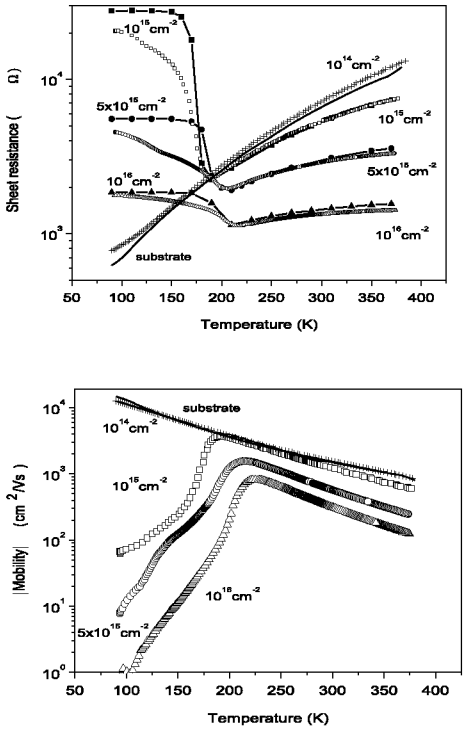

Figure 4: **a)** Sheet resistance as a function of measured temperature for a n-Si substrate (–) and for double sheet TIL/n-Si substrate for different implantation doses: $10^{14}cm^{-2}$ (+ experimental); $10^{15}cm^{-2}$(□ experimental; ■ ATLAS simulation); 5×10^{15} cm^{-2} (o experimental; ● ATLAS simulation) and 10^{16} cm^{-2} (Δ experimental; ▲ATLAS simulation) **b)** Mobility absolute value as a function of the measured temperature for a n-Si substrate (–) and for double sheet TIL/n-Si substrate for different implantation doses: $10^{14}cm^{-2}$ (+); $10^{15}cm^{-2}$(□); 5×10^{15} cm^{-2} (o) and 10^{16} cm^{-2} (Δ).

Where $F=G_t/(G_t+G_{C2})$, Gc_1 and Gc_2 are the sheet conductance of the layer 1 and layer 2 respectively, Gt is the transverse or limiting conductance and α is a geometric factor that takes into account the relative size between the contacts and the substrate size.

Same procedure was used with Vanadium implanted silicon. Fig 6 and 7 presents a comparison between the sheet resistance and the mobility of the V and Ti showing the shame shape in both variables but with differences in the temperature for the minimum on the resistivity and for the maximum in the mobility.

An important feature of the mobility is the change of its sign at low temperatures that happens for all the doses and all the PLM energies. Figure 8 presents this change for a $10^{16}cm^{-2}$ Ti sample annealed at 0.8 J/cm2. All the samples were N type for high temperature changing to P type at low temperatures.

The model used gives us the carrier density on the IB and its mobility. It is important to note that this density is almost constant until the minimum obtainable temperature in our cryostat, namely 7K. This semimetal behavior together with the low mobility p type defines clearly a half filled band which is not compatible with a conduction process based on isolated defects. The fact to have the sheet resistance minimum at different temperatures depending on the implanted element is also another argument indicating the IB formation

IV.- LIFETIME RECOVERY AND PHOTOCONDUCTIVITY

The former arguments prove the existence of the IB. However an IB without a recovery in the carrier lifetime is intrinsically useless. This recovery has been proved in (11) and (12) by measuring the photoconductive response. Figure 9 presents the spectral photoconductance normalized to the incident photon flux of a series of Ti implantations on a 3000Ω.cm substrate. The infrared substrate response is also plotted. In this last case the excess carriers are due to the generation on the superficial states combined with the high carrier lifetime typical of high resistance substrates (13).

Samples implanted at $10^{13}cm^{-2}$ shows a dramatic decrease in the photoconductivity which is related to the presence on the

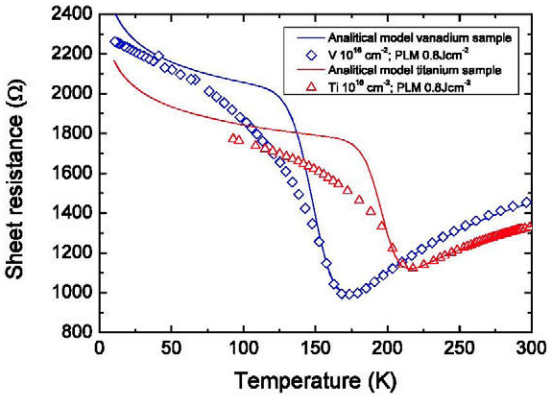

Figure 6: Comparison between the analytical model results and the measured values for the sheet resistance as a function of the temperature in the Ti implanted sample at 10^{16} cm^{-2} dose and the V implanted sample at 10^{16} cm^{-2} dose subsequently PLM processed at 0.8 Jcm^{-2}

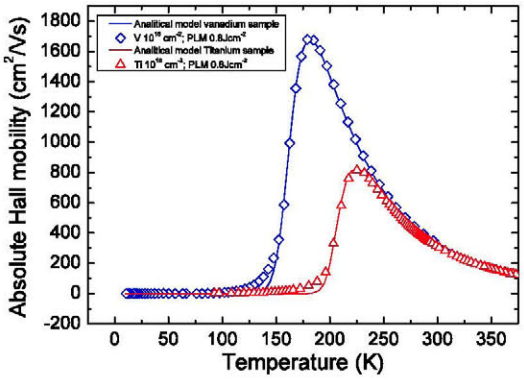

Figure 7: Comparison between the analytical model results and the measured values for the mobility as a function of the temperature in the Ti implanted sample at 10^{16} cm^{-2} dose and the V implanted sample at 10^{16} cm^{-2} dose subsequently PLM processed at 0.8 Jcm^{-2}.

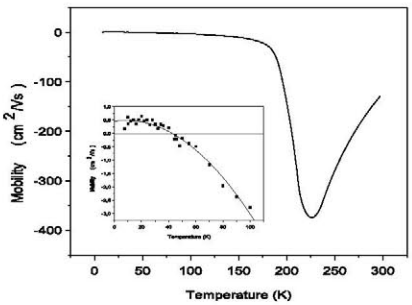

Figure 8: Hall mobility for a sample implanted with a dose of $10^{16}cm^{-2}$ and PLM at $0.8J/cm^2$ measured down to 7 K and showing p-type conductivity at low temperatures. Inset shows an enlargement of the mobility at low temperature.

silicon surface of a high quantity of deep levels. The Ti concentration for this dose is lower than the Mott limit and consequently they will have a very important recombination velocity. Contrarily as it can be assumed, an increment on the Ti concentration produces higher photoconductivity, i.e. a higher excess carrier concentration. Even with a dose of $10^{15}cm^{-2}$ we obtain higher photoconductivity than the substrate itself though in in a limited energy range. That means that not only we have recovered the mean free path of the electrons in the substrate because the recombination in the implanted zone has decreased but that the implanted layer is giving carriers to the substrate.

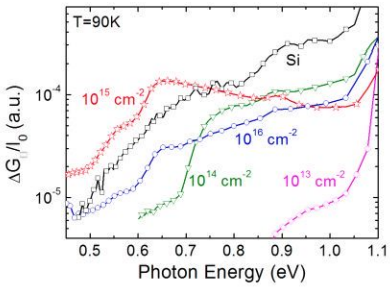

Fig 9: Normalized sheet photo-conductance versus photon energy for Ti implanted samples with doses from 1014 – 1016cm-2. Also shown 3000Ω.cm substrate sheet photoconductance

Figure 10 shows the sheet photoconductance for a 200Ωcm substrate and for the same substrate implanted with $10^{16}cm^{-2}$ V. As the substrate conductivity is now lower than the previous case the increase in photoconductance is due to the implanted V. It is important to note the very sharp photoconductance front at about 0.2eV. Also the coincidence for the implanted and non-implanted sample for energies higher than the fundamental Si absorption

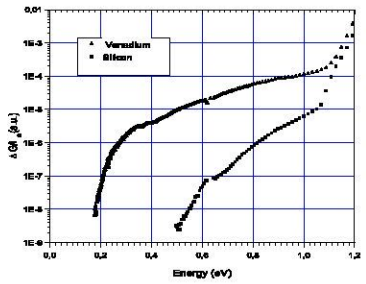

Fig 10: Sheet photoconductance for a V implanted sample and for the 200Ω substrate

V.- CONCLUSIONS

We present a model describing the electrical behaviour of V and Ti implanted layers on Si substrates. These implantations have been analysed using a variety of experimental techniques to determine the position of the impurity in lattice, the degree of cristallinity and so on. We conclude that a IB is formed and we develop an electrical model wich allow us to know the carrier concentration and the mobility of the IB.

Photoconductance measurements confirms the existence of the band and also that the lifetime is recovered being this lifetime higher in more impurified samples unlikely the deep level theory predicts. The photoconductance of V samples extend down to 0.2eV having a sharp and very defined front.

ACKNOWLEDGEMENTS

Authors would like to acknowledge the CAI de Técnicas Físicas of the Universidad Complutense de Madrid for the ion implantations and metallic evaporations. This work was partially supported by the Project NUMANCIA II (Grant No. S-2009/ENE/1477)

funded by the Comunidad de Madrid. Research by E. García-Hemme was also supported by a PICATA predoctoral fellowship of the Moncloa Campus of International Excellence (UCM-UPM). J. Olea and D. Pastor thanks Professor A. Martí and Professor A. Luque for useful discussions and guidance and acknowledge financial support from the MICINN within the program Juan de la Cierva (JCI-2011-10402 and JCI-2011-11471), under which this research was undertaken.

REFERENCES

(1) A. Luque and A. Mart_ı, Phys. Rev. Lett. 78, 5014–5017 (1997).
(2) Luque, A; Marti, A; Antolin, E; et al. Physica b-Condensed Matter 382- 1-2, 320-327 (2006)
(3) Krich, Jacob J.; Halperin, Bertrand I.; Aspuru-Guzik, Alan J.Appl. Phys. 112 013707 (2012)
(4) A. Karoui Appl. Phys. Lett. 101, 236101 (2012)
(5) Bremner, S.P.; Levy, M.Y.; Honsberg, C.B. Appl. Phys. Lett. 92 - 17 171110-1-3 (2008)
(6) Persans, Peter D.; Berry, Nathaniel E.; Recht, Daniel; et al. Appl. Phys. Lett. 101 – 11 (2012)
(7) Sanchez, K.; Aguilera, I.; Palacios, P.; et al. Phys. Rev. B 79 - 16 (2009)
(8) Olea, J.; Pastor, D.; Toledano-Luque, M.; et al. J. Appl. Phys 110 6 (2011)
(9) (9) Pastor, D.; Olea, J.; del Prado, A.; et al. Sem. Science and Technol. 26 11 (2011)
(10) D. Pastor, J. Olea, I. Mártil, G. González Díaz, A. Muñoz and A. Climent Font. J. Appl. Phys 112(2012) 113514
(11) Garcia-Hemme, E; Garcia-Hernansanz, R; Olea, J; Pastor, D; del Prado, A; Martil, I; Gonzalez-Diaz, G Appl. Phys. Lett. 101-19 (2012)
(12) Antolin, E; Marti, A; Olea, J; Pastor, D; Gonzalez-Diaz, G; Martil, I; Luque, A. Appl. Phys. Lett. 94 - 4 2009
(13) Muller W, Monch W. Phys Rev Lett 25 5 (1971) 250